Comparative study of immunocytological, immunohistochemical and in-situ hybridization methods in small ruminant neonatal mortality

Sevil Atalay VURAL[1,a,✉], Rıfkı HAZIROĞLU[1,b], Osman KUTSAL[1,c], Gözde YÜCEL TENEKECİ[1,d], Arda Selin TUNÇ[1,e], Yanad ABOU MONSEF[2,f], Ozan AHLAT[1,g], Kürşat FİLİKCİ[3,h], Özgür ÖZÖNER[4,i], Oya Burçin DEMİRTAŞ[1,j]

[1]Ankara University, Faculty of Veterinary Medicine, Department of Pathology, Ankara, Türkiye; [2]Université de Toulouse, Ecole Nationale Vétérinaire de Toulouse, Laboratory of Anatomic Pathology, Toulouse, France; [3]Harran University, Faculty of Veterinary Medicine, Department of Pathology, Şanlıurfa, Türkiye; [4]Siirt University, Faculty of Veterinary Medicine, Department of Pathology, Siirt, Türkiye.

[a]ORCID: 0000-0003-2111-3381; [b]ORCID: 0000-0002-1134-3581; [c]ORCID: 0000-0003-3599-6867; [d]ORCID: 0000-0002-2586-8346; [e]ORCID: 0000-0002-4813-7626; [f]ORCID: 0000-0002-4929-9395; [g]ORCID: 0000-0002-2580-8140; [h]ORCID: 0000-0001-9710-9480; [i]ORCID: 0000-0001-7354-0655; [j]ORCID: 0000-0003-0850-2374

ARTICLE INFO

Article History
Received : 01.08.2024
Accepted : 17.02.2025
DOI: 10.33988/auvfd.1526014

Keywords
Immunocytochemistry
Immunohistochemistry
Infection
In situ hybridization
Neonatal small ruminant

✉Corresponding author
sevilvural@yahoo.com

How to cite this article: Vural SA, Hazıroğlu R, Kutsal O, Yücel Tenekeci G, Tunç AS, Abou Monsef Y, Ahlat O, Filikci K, Özöner Ö, Demirtaş OB (2025): Comparative study of immunocytological, immunohistochemical and in-situ hybridization methods in small ruminant neonatal mortality. Ankara Univ Vet Fak Derg, 72 (3), 277-286. DOI: 10.33988/auvfd.1526014.

ABSTRACT

It was aimed to identify diseases using immunocytochemical, immunohistochemical, and in-situ hybridization methods, to determine sensitivity and specificity among these techniques, and to highlight their advantages and disadvantages for certain respiratory (*Mycoplasma pneumonia, Pasteurella spp.,* Respiratory syncytial virus, Parainfluenza virus 3) and enteric (Coronavirus, Rotavirus, *Escherichia coli, Clostridium spp.*) agents. The obtained results were compared, and although the immunocytochemical method was found to be the fastest, immunohistochemistry was proved to be the most reliable method. Our other aim was to establish pathological diagnostic panels for neonatal infections. All antibodies tested were found to be positive except for *Pasteurella multocida*. The immunohistochemical findings of the study indicate that nearly all cases that result in death involved mixed infections.

Introduction

Breeding ruminants strongly contributes to the country's economy both in Türkiye and worldwide. These animals provide basic dietary needs with meat, milk, and their products, or complement the textile and leather industry with their skin and coat. Especially small ruminants play an important role in food diversity, mainly in rural areas, due to their contributions to the meat and dairy industry and their capability of reproducing. Having healthy offspring and protecting the high quality of the breed has importance in the continuity of such a substantial species. After birth, newborns transfer to an unprotected, risky environment from the warm and safe atmosphere of the uterus, being most vulnerable on the day of birth (10, 12, 17, 18).

Pathogens of the digestive and respiratory tracts are the foremost causes of neonatal deaths (4, 10, 12, 14, 16). Neonatal enteritis is one of the most common diseases in

small ruminants less than 3 weeks old, with a high morbidity and mortality rate (12). Being a syndrome known to be complex and multifactorial, the disease can occur due to a number of reasons, such as herd management system, hypothermia, hyperthermia, hunger, environmental factors, insufficient colostrum intake, and infectious agents (2). According to the study by Holmoy et al. (2017), 80% of neonates die within 2 days; 41% in 24 hours, and 27% in the first 3 hours. This lifespan is set as 5 weeks in some studies. In herds of sheep, the most common reason for neonatal deaths is infectious diseases, with a rate of 37%, with these being septicemia (48%), pneumonia (25%), gastroenteritis (22%), and other (5%). Lots of enteric pathogens are related to diarrhea in neonates, but agents most commonly seen are *Escherichia coli*, *Salmonella spp*., and *Clostridium perfringens* as bacteria; rotavirus, coronavirus, herpesvirus, and adenovirus as viruses; and *Cryptosporidium spp.* as protozoans (9, 10, 15, 18). Due to the fact that there are prophylactic methods and treatments developed for most of these pathogens, the etiological diagnosis of enteritis has significant importance (4, 8).

In this article, diagnosing diseases using immunocytochemical (ICC), immunohistochemical (IHC), and in-situ hybridization (ISH) methods, determining the sensitivity and specificity of these methods, and revealing their advantages and disadvantages in the diagnostic process, and by this, determining the quickest, most reliable, and most practical method for early diagnosis and updating information on the factors that cause death was aimed. Also, creating pathological diagnostic panels in newborns in our department, bringing them into active use in routine diagnosis, and preventing economic loss for the breeders was another important purpose.

Materials and Methods

Study material (n: 44) consisted of lungs, mediastinal/ mesenteric lymph nodes, and intestinal tissues of animals (kid n: 8 and lamb n: 36) of different breeds (n: 15 Merino, n: 5 Karaman, n: 1 Angora, Suffolk, and Sakız, n: 21 breed unknown) and ages (0-60 days) brought to the Department of Pathology for necropsy.

Cytochemical/Immunocytochemical Examinations: Cytological touch slides were prepared from lungs (affected areas and/or areas of bronchi) and mediastinal/mesenteric lymph nodes and stained with both Diff Quick and the indirect immunoperoxidase technique using primary antibodies simultaneously.

Immunohistochemical Examinations: Fixated tissues in 10% buffered formalin (pH: 7.2) were put in the routine tissue fixation device (Epredia/Thermo Scientific STP 120-2) and blocked in paraffin (Epredia/Thermo Scientific Histostar A81000001). 5 µm thick sections were prepared (Epredia/Thermo Scientific HM355S) and stained with hematoxylin eosin (HE) and avidin-biotin complex peroxidase (ABC-P) technique, according to the kit procedure. The primary antibodies used were *Mycoplasma pneumonia* (rabbit polyclonal, 1:100 NovusBio), *Pasteurella multocida* (pig, 1:200, ATCC), *Escherichia coli* (rabbit polyclonal, 1:1000, NovusBio), *Clostridium spp.* (rabbit polyclonal, 1:100, BioRAD), parainfluenza 3 (Mouse Ig1, 1:100, LsBio), respiratory syncytial virus (RSV) fusion protein (Mouse IgG2B, 1:200, Invitrogen), rotavirus (Mouse A2, 1:100, LsBio), and coronavirus (Mouse IPV3-70, 1:300, LsBio). Properties of the antibodies are given in Table 1. The immunohistochemical (IHC) presence of antigens was measured semiquantitatively using a x40 objective by at least two different experts and evaluated as follows: (+) 1-10 immunopositivity; (++) 10-50 immunopositivity; (+++) more than 50 immunopositivity in 10 different microscopical fields. As a negative control, mouse IgG serum was used. For IHC, 3-amino-9-ethylcarbazole (AEC) chromogen solution and Gill's hematoxylin were used, and slides were sealed with glycer gel.

Table 1. Antibodies used in the study and their properties.

Marker	Specie	Clone	Dilution	Brand	Antigen Retrieval
Mycoplasma pneumonia (M. pneumonia)	Rabbit	Polyclonal	1:100	NovusBio	Citrate buffer (pH:6.0)
Pasteurella multocida (P. multocida)	Pig	Polyclonal	1:200	ATCC	Citrate buffer (pH:6.0)
Escherichia coli (E. coli)	Rabbit	Polyclonal	1:1000	NovusBio	Citrate buffer (pH:6.0)
Clostridium spp.	Rabbit	Polyclonal	1:100	BioRAD	Citrate buffer (pH:6.0)
Parainfluenza 3	Mouse	IgG1	1:100	LsBio	Citrate buffer (pH:6.0)
RSV Fusion Protein	Mouse	IgG2B	1:200	Invitrogen	Citrate buffer (pH:6.0)
Rotavirus	Mouse	A2	1:100	LSBio	Citrate buffer (pH:6.0)
Coronavirus	Mouse	FIPV3-70	1:300	LSBio	Citrate buffer (pH:6.0)

DOI: 10.33988/auvfd.1526014

In-Situ Hybridization Examinations: The sections were stained according to the kit (ZytoDot 2C CISK Implement Kit, Zytovision) procedure. Probes labeled with digoxigenin (Table 2) matching the disease, and for control purposes, positive tissues and/or control probes were used.

Statistical Analysis: In 10 different areas at x40 (0.2 mm² per field) magnification, immunopositivities were counted [Leica Application Suite Version 4.9.0 (Build 129) Leica microsystem (Switzerland)]. The Kruskal-Wallis Test was used for statistical calculations between groups; the Dunn Test for testing between individual groups; and the IBM SPSS 21.0 (SPSS Inc., Chicago IL, USA) program to perform statistical calculations.

Results

Macroscopic Findings: A foamy to bloody exudate was seen in tracheal lumens and on the cut surface of lungs (n: 28). The pleura was thickened with fibrin (n: 13) (Figure 1a). Yellowish pus was observed on cut sections (n: 5), and an abscess (n: 1; 1 cm diameter). The lungs had crepitation (n: 9). Mediastinal lymph nodes were enlarged; their cut sections were moist (n: 18) and/or mottled grey/reddish (n: 4). Reddish color changes (n: 2) and hyperemia were observed in intestinal serosa (n: 2) (Figure 1b). Mucous content adhered to the mucosa, along with non-viscous, yellowish, or hard content in lumens. Adhesions along with intussusception were noted (n: 1). Mesenteric lymph nodes were enlarged, and the cut sections appeared moist (n: 27).

Table 2. Probes used in the study and their properties.

PROBE	Sequence	Oligo-base Type	Base Amount	Molecular Weight	GC Content	Ext.Cofficient (L / (mole.cm))
RSV (F)	5'- /5DigN/ TGA TAA GCT GCA GTC GAA TCC/ 3Dig_N/ -3'	DNA	21	7.907.9	47.6%	230.500
RSV (R)	5'- / 5DigN/ CTG AAC CAG ATC GTA ACG GC/3Dig_N/ -3'	DNA	20	7.588.7	55.0%	220.600
***E. coli* (F)**	5'-/5DigN/AAT AAA TCA TAA GTC AGT AGT AGA CCA TGT /3Dig_N/-3'	DNA	30	10.723.8	30.0%	343.600
***E. coli* (R)**	5'-/5DigN/AAT AAA TCA TAA TAA GCT GGT ATT GAT GCA /3Dig_N/ -3'	DNA	30	10.738.8	26.7%	340.600
***Rotavirus* (F)**	5-/5DigN/GAC GGV GCR ACT ACA TGG T/3Dig_N/ -3'	DNA	19	7.344.9	58.8%	213.113
***Rotavirus* (R)**	5'-/5DigN/GTC CAA TTC ATN CCT GGT G/3Dig_N/ -3'	DNA	19	7.252.3	50.0%	201.700
***Pasteurella multocida* (F)**	5'-5DigN/AGA AAG CAC ATG ACC AAA GGG /3Dig_N/-3'	DNA	21	7.984	47.6%	249.800
***Pasteurella multocida* (R)**	5'-/5DigN/GCA GCT ACT CGC AGA AGG TT/3Dig_N/ -3'	DNA	20	7.619.7	55.0%	218.800
***Mycoplasma pneumonia* (F)**	5'-/5DigN/ACT CCT ACG GGA GGC AGC AGT A/3Dig_N/-3'	DNA	22	8.247.2	59.1%	244.400
***Mycolasma pneumonia* (R)**	5'- /5DigN/TGC ACC ATC TGT CAC TCT GTT AAC CTC /3Dig_N/ -3'	DNA	27	9.599	48.1%	265.300

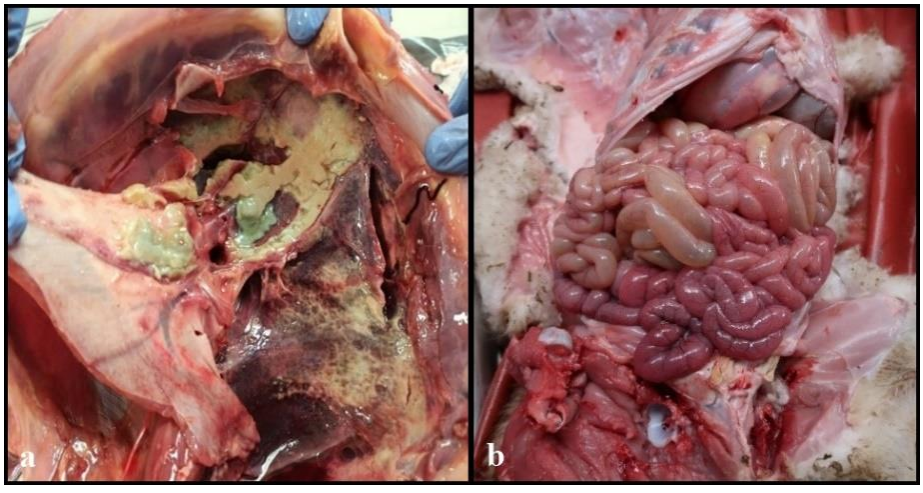

Figure 1. Macroscopic appearance: thickened pleura (a), intestines with reddish color changes in the serosa and gas-filled lumens (b).

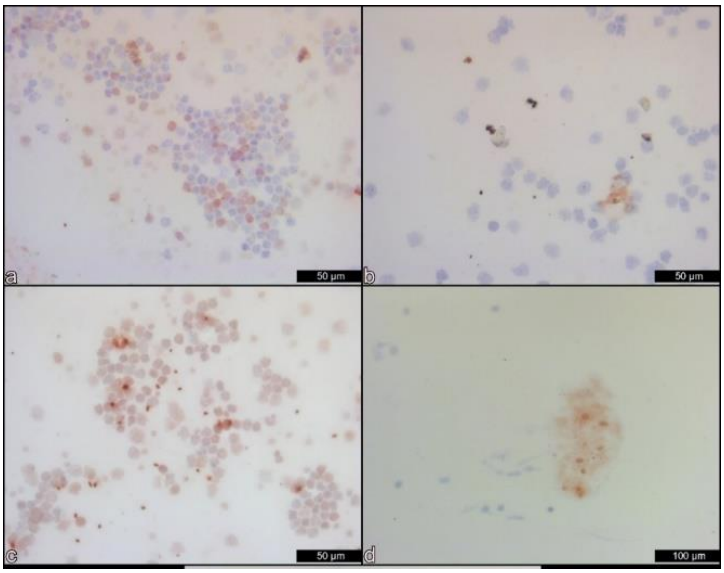

Figure 2. Rotavirus (a), *Clostridium spp*. in macrophages (b) and *E. coli* (c) immunopositivity in mesenterial lymph nodes; *M. pneumonia* (d) immunopositivity in mediastinal lymph nodes, ICC.

Cytochemical/Immunocytochemical Findings: In the examinations, inflammatory cells, especially lymphocytes and macrophages, were encountered. Rotavirus (Figure 2a), *Clostridium spp.* (Figure 2b), and *E. coli* (Figure 2c) were detected either free and/or within the cytoplasm of macrophages and lymphocytes. *M. pneumoniae* (Figure 2d) was found within the cytoplasms of macrophages and lymphocytes, while parainfluenza 3 was identified as a free agent in the lung exudates. In the mediastinal lymph nodes, no positivity was detected for coronavirus, RSV, or *P. multocida* antibodies.

Histopathological Findings: Microscopically, fewer or more neutrophils and leukocytes were seen only in the alveoli (n: 2; alveolitis); in the bronchi and bronchioli (n: 1; purulent bronchitis); or in both the alveoli and bronchi/bronchioli (n: 2; acute catarrhal bronchopneumonia, n: 2; subacute catarrhal bronchopneumonia; n: 4; subacute bronchopneumonia; n: 3; purulent bronchopneumonia) (Figure 3a, 3b). Also, necrosis was seen (n:2; necrotic bronchopneumonia). In addition, fibrin accumulations were found in both alveoli and bronchi/bronchioli lumens, along with pleura & interlobular septae (n: 5; fibrinonecrotic bronchopneumonia) and enlarged lymphatics. In some cases, bronchopneumonia accompanied only by fibrin was observed (n: 5). It was accompanied by purulent inflammation in a single case (n: 1; fibrinopurulent bronchopneumonia). In a few cases, although the alveoli were empty, cellular infiltrate with a majority of mononuclear cells was observed in the peribronchial/bronchiolar and perivascular areas. In some cases, the interalveolar region was thickened due to varying amounts of inflammatory cells (n: 6; interstitial pneumonia) (Figure 3c). In one case, granulomatous areas dominated the field (n:1; granulomatous pneumonia). Cases in which atelectasis, hyperemia, and/or edema (n: 6) were observed along with emphysema, where the inflammation had not started yet, were also encountered.

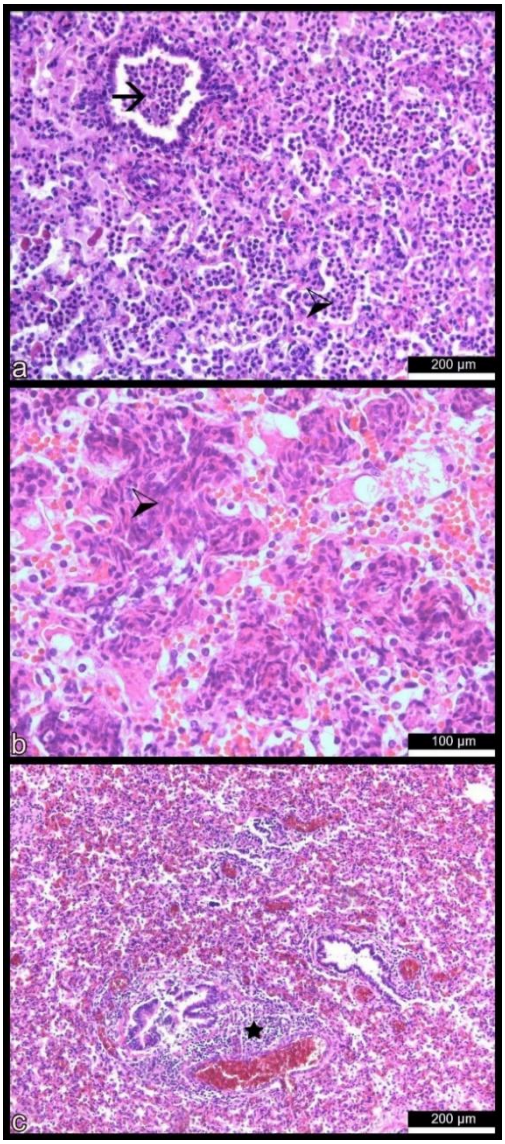

Figure 3. Purulent bronchopneumonia (a, b), neutrophil leukocytes in the bronchiolar lumen (arrow) and alveolar lumens (arrowhead), *M. pneumoniae*; interstitial pneumonia (c), peribronchiolar and perivascular mononuclear cell infiltration (stars), parainfluenza virus, HE.

DOI: 10.33988/auvfd.1526014

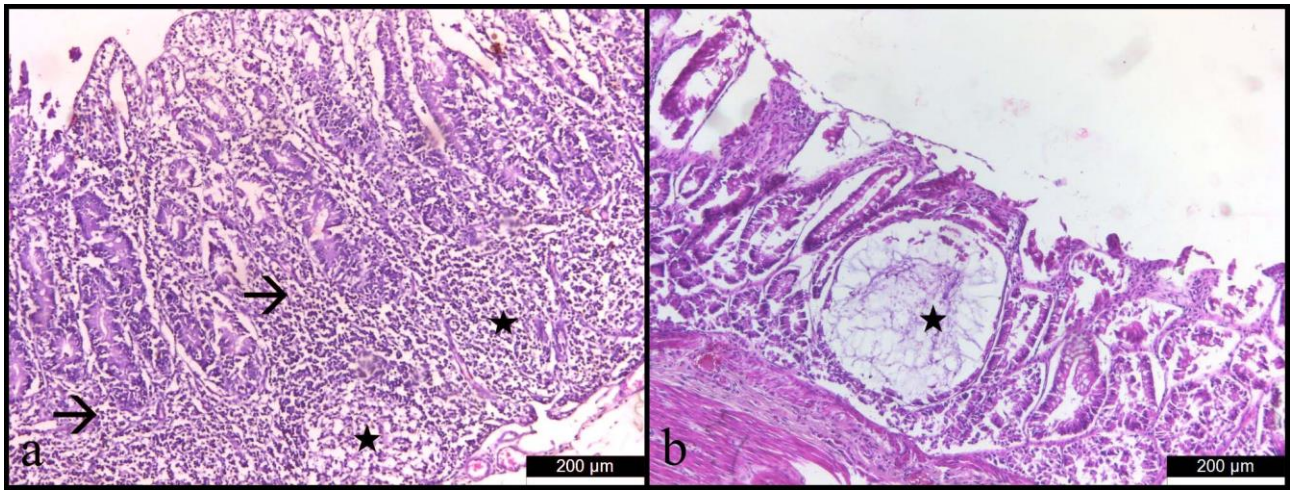

Figure 4. Subacute enteritis (a), *Clostridium spp*., inflammatory cell infiltrations (arrows) and hyperplastic lymphoid follicles (stars); cystic Lieberkühn glands (b), cystic structure (asterisk), rotavirus, HE.

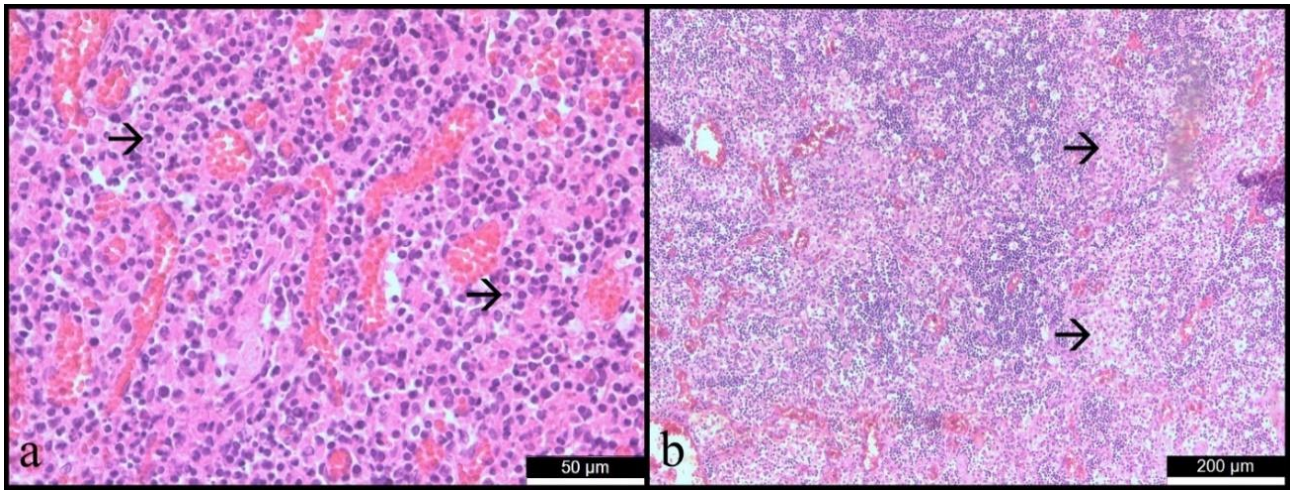

Figure 5. Sinus catarrh (a), neutrophils in sinuses (arrows), *M. pneumoniae*; necrotic lymphadenitis (b), necrotic lymphoid follicles (arrows), *E. coli*, HE.

In most of the intestines examined, inflammatory cell infiltrates consisting of a few neutrophils, leukocytes, a greater number of plasma cells, lymphocytes, and macrophages were observed between the glands in the lamina propria (n: 13). Changes in the ileum were accompanied by hyperplasia of aggregate lymph follicles (Figure 4a). Necrotic material, secretion, and a small number of neutrophil leukocytic cell infiltrations accompanied by cystic dilated changes in the crypts (n:1), inflammation only in the jejunum (n:1; jejunitis), and cystic changes only in the Lieberkühn glands (n:1) (Figure 4b) were observed. Parasites (n: 4; parasitic enteritis) were observed in intestinal tissues of 4 out of 16 animals. Lymphadenitis simplex (n: 14), sinus catarrh (n: 2) (Figure 5a), and necrotic lymphadenitis (n: 3) (Figure 5b) were seen in the mesenteric lymph nodes.

Immunohistochemical Findings: In all cases, lungs, intestinal sections, and existing mediastinal/mesenterial lymph nodes were stained with the relevant antibodies.

Lungs: *P. multocida* was negative for all lung tissues. *M. pneumonia* (n: 17, Figure 6a), parainfluenza 3 (n: 20, Figure 6b), RSV (n: 4, Figure 6c), and *E. coli* (n: 35, Figure 6d) were found to be positive.

Mediastinal Lymph Nodes: Immunohistochemical staining was performed (n: 20/22). No positivity was seen for *P. multocida* and RSV antibodies. *M. pneumoniae* (n: 1), parainfluenza 3 (n: 10, Figure 6e), and *E. coli* (n: 5, Figure 6f) were found positive in capsule, cortex, and/or medulla, free and/or in macrophages.

DOI: 10.33988/auvfd.1526014

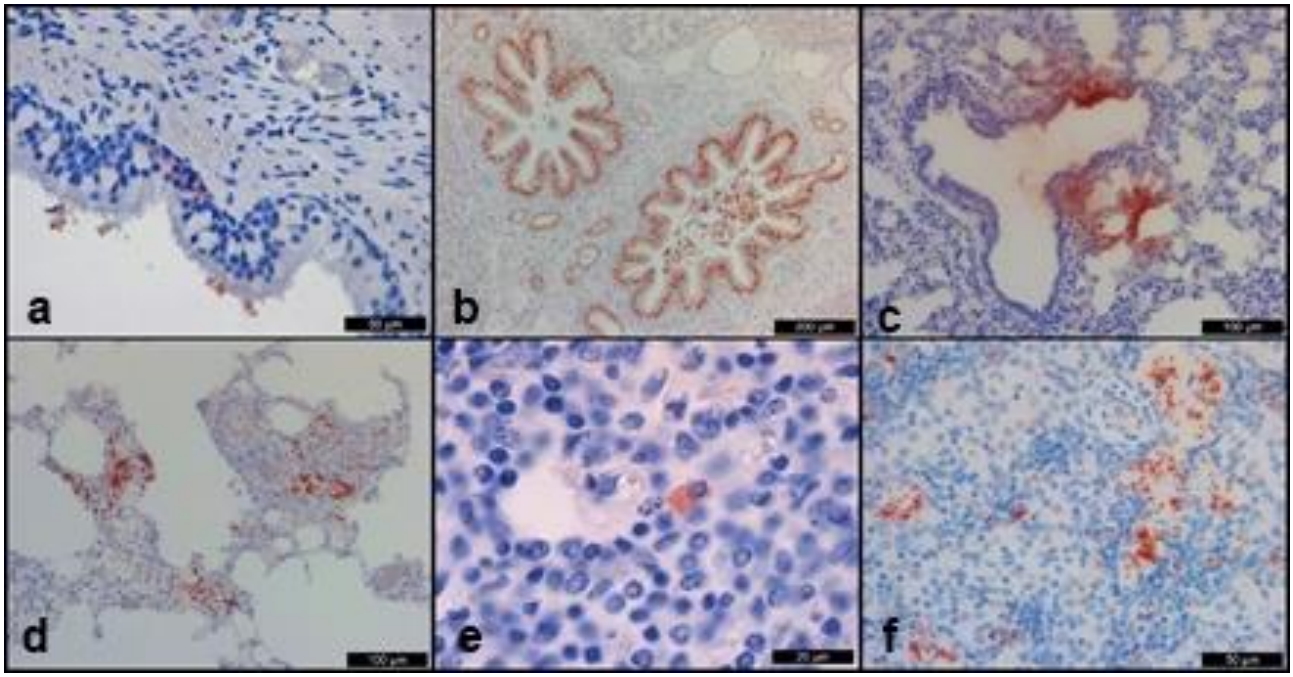

Figure 6. Immunopositivity of *M. pneumoniae* (a); parainfluenza 3 (b); RSV (c); and *E. coli* (d); parainfluenza 3 (e); and *E. coli* (f) seen free, in epithelial cells, and/or phagocytosed in macrophages, IHC.

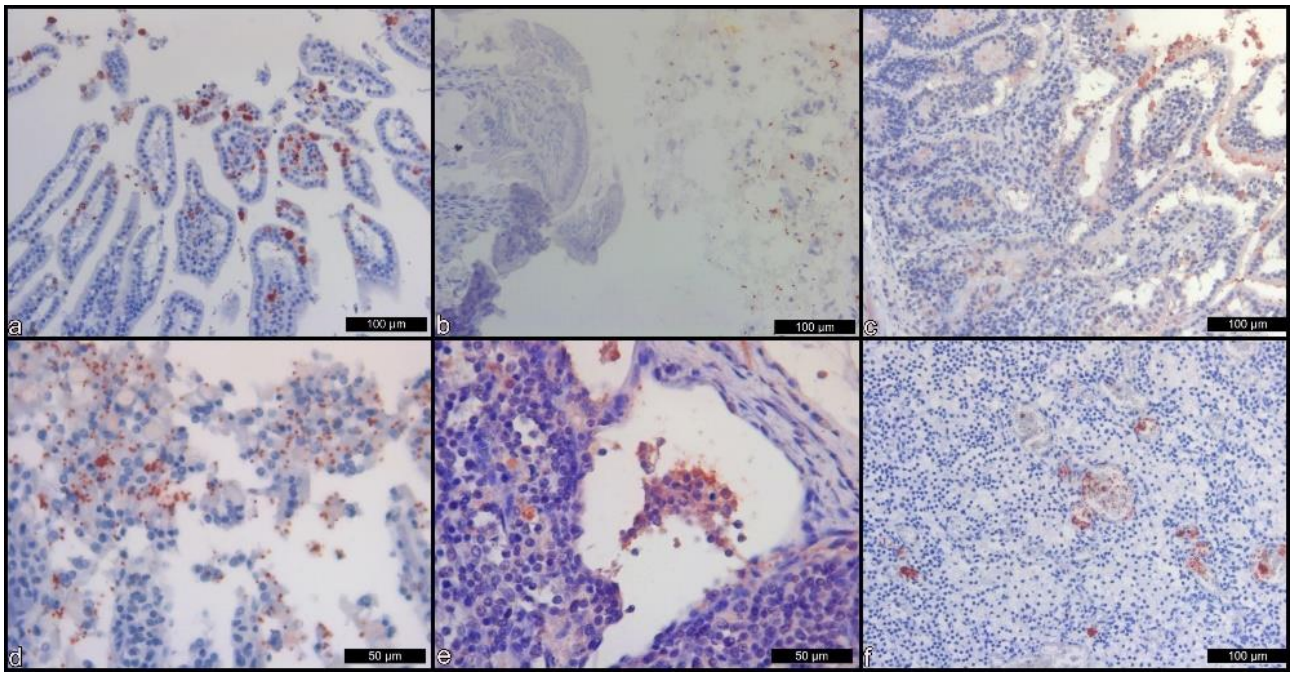

Figure 7. Rotavirus (a), coronavirus (b), *Clostridium spp.* (c), *E. coli* (d), and *Clostridium spp.* (e) immunopositivity in epithelial cells or macrophages, also *E. coli* positivity in the vascular lumens (f), IHC.

Intestines: Rotavirus (n: 11, Figure 7a) was found positive in the jejunum, ileum, colon, and cecum; coronavirus (n: 3, Figure 7b) in the duodenum, colon, and cecum; *Clostridium spp.* (n: 33, Figure 7c) in all intestines; and *E. coli* (n: 35, Figure 7d) in the duodenum, ileum, and cecum. The positivities were generally seen on villus surfaces, in the cytoplasm of epithelial cells, and in macrophages.

Mesenteric Lymph Nodes: Immunohistochemical staining was performed (n: 29/31). No positivity was seen for the coronavirus antibody, but rotavirus (n: 3), *Clostridium spp.* (n: 19, Figure 7e), and *E. coli* (n: 11, Figure 7f) positivities were seen in the cytoplasms of macrophages, in the cortex, and in the vascular lumens.

DOI: 10.33988/auvfd.1526014

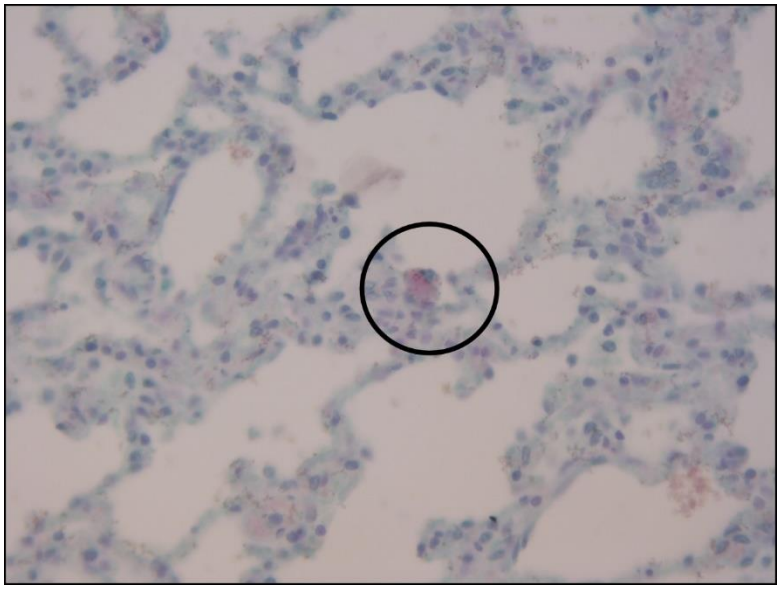

Figure 8. *E. coli* positivity in the lung (circle), CISH.

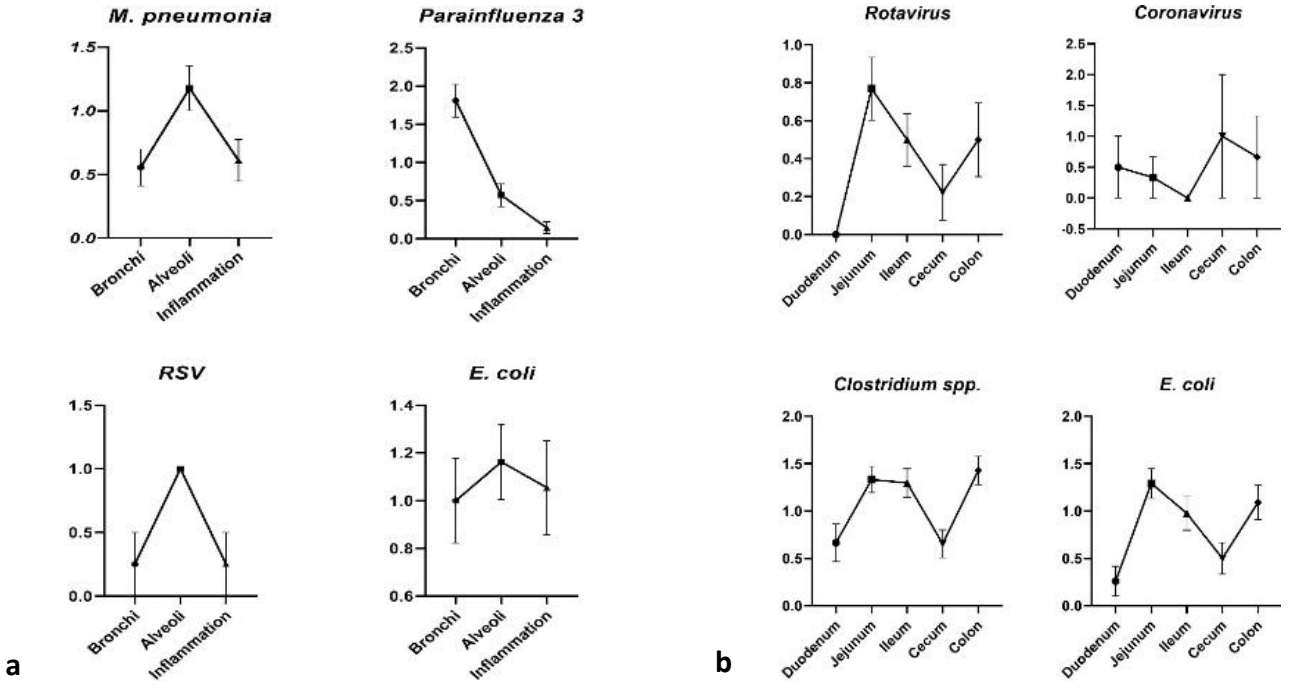

Figure 9. Statistical immunopositivity rates of the agents seen in the lungs (a) and intestines (b).

In Situ Hybridization Findings: In the staining results, *E. coli* (n: 4) (Figure 8) and parainfluenza 3 virus (n: 2) were detected in the lungs, while mild positivity was detected for *E. coli* (n: 4) and rotavirus (n: 2) in the intestines; no positivity was observed in any of the relevant regional lymph nodes.

Statistical Findings

Lungs: In statistical examinations of the regions, immunopositivity was seen, and a statistically significant difference was observed for *M. pneumoniae* (P=0.021). When the settlements are compared among themselves, a difference was observed between bronchi and alveoli, but none between bronchial inflammation and alveolar inflammation. For parainfluenza 3, a statistical difference was observed between settlements (P<0.001). When compared, although there was a statistical difference between the staining rate in the bronchi and both the alveoli and inflammation, no statistical difference was observed between the staining rates in the inflammation and alveoli. No statistically significant difference was observed for RSV (P=0.143) and *E. coli* (P=0.536) (Figure 9a). Statistical evaluation could not be made for the *P. multocida* due to a lack of samples.

Intestines: A statistically significant difference was observed for rotavirus (P=0.017). When the intestinal segments were compared, only a difference was seen between the duodenum and jejunum. A statistically significant difference was detected between locations and staining intensities for Clostridial factors (P<0.001). When the locations were compared, a statistically significant difference was seen between duodenum-jejunum, duodenum-colon, jejunum-cecum, and cecum-colon pairings. For E. coli, a statistically significant difference was observed when the staining intensities were compared (P<0.001). When the intestinal sections were compared, a statistically significant difference was detected between duodenum-jejunum, duodenum-ileum, duodenum-colon, and jejunum-cecum. There was no statistically significant difference for the coronavirus (P=0.964). Also, since the in situ hybridization staining results were few in number and mild in intensity, significant results could not be obtained. They were excluded from statistical evaluations (Figure 9b).

Discussion and Conclusion

The bacterial bronchopneumonias include *Mycoplasma spp.*, *Mannheimia haemolytica*, *Histophilus somni*, and *Pasteurella multocida*. *M. haemolytica* can cause septicemia without pneumonia in lambs younger than 2 months (3). In this study, *M. haemolytica* antigen was detected more prominently in cases diagnosed with fibrinous and/or fibrinonecrotic bronchopneumonia. When evaluated in general, it is concluded that, unlike the common approach, it would be appropriate to evaluate fibrinous pneumonias first for *M. haemolytica* and then for other fibrinous bronchopneumonia agents (*Mycoplasma spp.* and *Pasteurella spp.*). In the study of Yener et al. (2005), bacterial agents were detected in 32 of 42 pneumonia lung tissues. These are *P. haemolytica* (38.09%), *Mycoplasma spp.* (28.57%), *Staphylococcus aureus* (16.66%), *Klebsiella pneumoniae* (11.90%), *Moraxella spp.* (4.76%), *Bacillus spp.* (4.76%), and *P. multocida* (2.38%). The presence of parainfluenza 3 (PI3) viral antigen was found in 28 of these samples. However, no positivity was observed in tissues without pneumonia. In our study, in addition to lungs with pneumonia, mild PI3 positivity was also found in sections showing emphysema and atelectasis. The location of PI3 immunopositivity in the lung tissue in the study was mostly similar to other studies (1, 3, 6, 11, 19). In addition, it was noticed that it was found free or phagocytosed by macrophages in the interstitial area, interlobar septa, and vascular surroundings. In addition, this study detected the presence of PI3 viral antigen and *E. coli* immunopositivity in the mediastinal lymph nodes. It was noted that PI3 infection usually occurs as a mixed infection with other factors. These include mainly *M. pneumoniae* and *E. coli*, and to a lesser extent respiratory synctial virus (RSV) and *P. multocida*. Therefore, histopathological diagnoses vary. The most prominent findings of PI3 infection are bronchiolitis and mild bronchitis. In the acute period, eosinophilic, intracytoplasmic inclusion bodies are seen in the bronchus, bronchiole, alveolar epithelial cells, and alveolar macrophages. BRSV together with PI3 should also be considered in cases of necrotic bronchiolitis (3). In this study, similar to the study by Yener et al. (2005), no inclusion bodies were found, no matter how acute the infection was. Within the scope of this study, the incidence of PI3 comes second, especially *E. coli*. In future studies, it would be appropriate to investigate in detail which strains of *E. coli* are involved in both lung and intestinal infections in newborn small ruminants and similarly, which species in the genus *Clostridium* cause intestinal infections. The most striking finding of BRSV infection is bronchiole and alveolar epithelial syncytia formation along with bronchointerstitial pneumonia. Syncytia and intracytoplasmic eosinophilic inclusion bodies are evident in the early stages (3). In this study, syncytia formation and inclusion bodies were not noticed in RSV immunopositive cases. It has been determined that the localization of RSV is similar to PI3. In *Mannheimia haemolytica* infection, the appearance of multinucleated macrophages around the fibrin in the alveoli may lead to a false diagnosis of RSV infection (3). In this study, RSV viral antigen was found in bronchiolar and alveolar epithelial cells, alveolar macrophages, and macrophages located in the interstitium. Chronic bronchopneumonia (atypical or chronic nonprogressive pneumonia) is common in lambs and kids, and *Mycoplasma ovipneumoniae*, *M. haemolytica*, and PI3 have been detected in its etiology (17). In this study, similar to other studies, *M. pneumoniae* antigen was detected on the bronchial/bronchiolar/alveolar epithelial surface and/or free or in desquamated epithelial cells in their lumens and in alveolar macrophage cytoplasms. Although *M. pneumoniae*, *E. coli*, RSV, and PI3 immunopositivity were detected in some lung sections, it was noticed that the pneumonia had not yet formed. We can relate this situation to the amount of agent, pathogenicity, duration of infection, and individual factors. In this study, unlike others, immunocytochemical staining was performed on touch slides prepared from lung tissue, mediastinal and mesenterial lymph nodes, and successful results were obtained. Following immunocytochemical examinations, *M. pneumoniae* was found in mediastinal lymph nodes and PI3 in lung tissues; rotavirus and *Clostridium spp.* from mesenterial lymph nodes and *E. coli* immunopositivity drew attention. Thus, immunocytological and immunohistochemical methods have again shown their importance in rapid diagnosis.

DOI: 10.33988/auvfd.1526014

Enterotoxigenic *E. coli* (ETEC), rotavirus, *C. perfringens* type B, and *Cryptosporidium parvum* are the main etiologies of neonatal diarrhea in small ruminants (13, 18). In this study, rotavirus, *Clostridium spp.*, and *E. coli* immunopositivity were found in the intestinal sections, especially jejunum, ileum and colon and mesenterial lymph nodes. Enterotoxigenic *E. coli* can cause more severe infections together with rotavirus (18). Thus, it was concluded that *Clostridium spp.* and *E. coli* pathogens, alone or together, were responsible for neonatal deaths in small ruminants. It has been reported that coronavirus infection was seen older than three months (7). In this study, the presence of coronavirus antigen was noticed, especially in the intestinal content (colon) and duodenum, unlike the previous research (15).

In our ISH examinations, due to insufficient positivity, it was not foreseen to be evaluated as a method that should be used in the rapid and routine diagnosis of the disease (5). In the stainings performed, both positive controls and ICC and IHC positive samples were repeated, especially the staining method, to eliminate possible kit and/or method drawbacks. Considering all these results, it has been determined that *Mycoplasma pneumonia*, *Escherichia coli*, parainfluenza virus 3, and respiratory syncytial virus, which are respiratory agents, and *Escherichia coli*, *Clostridium spp.*, coronavirus, and rotavirus, which are enteric agents, are still active in our country, apart from Pasteurella multocida, which is one of the respiratory agents. It was determined that neonatal deaths were not caused by a single agent alone but mostly occurred after mixed infection. In addition, the creation of immunohistochemical diagnostic panels against neonatal infections specified in the aims of the study was achieved. In addition, immunohistochemical and molecular (PCR, ELISA, etc.) techniques are frequently used in literature, and immunocytochemical studies are almost non-existent. In this study, immunocytochemical, immunohistochemical, and in situ hybridization methods were used; comparisons were made between the methods according to the results obtained after these stainings, and although the immunocytochemical method was determined to be the fastest-yielding method, immunohistochemistry was the one that gave the most reliable results. In the presentation of this article, with the results obtained by using a limited number of antibodies in the respiratory and digestive systems, the expected targets were achieved, excluding ISH, and a relevant diagnostic panel (HP, ISC, and IHC) was created, which can be actively used in diagnosis in our laboratory in the future.

Acknowledgements

We would like to thank Prof. Dr. Ender YARSAN, the Phd student of our department Kübra ÇETİN ALTUN and veterinarian Kamil ALPLER, along with our lab technician Habibe DÖNMEZ for technical support; Prof. Dr. Halit KANCA for his contributions in providing materials. In addition, I would like to thank Veterinarian Yeşim YILMAZ and Cengiz YILMAZ, and also Assoc. Prof. Dr. Funda TERZİ for her help in finding Parainfluenza 3 positive blocks.

Financial Support

This research has been suported by Ankara University Scientific Research Projects Coordination Office as a Guided Infrastructure Project, within the content of the project number 21A0239003.

Ethical Statement

This study does not present any ethical concerns.

Conflict of Interest

The authors declared no conflict of interest.

Author Contributions

SAV planned and conceived the idea of the research, along, with scientific support throughout the project. GYT, AST, YAM, OA, KF, ÖÖ, and OBD took part in collecting material, data and necessary stainings with pre-evaluation. RH and OK helped writing the article with their profound experience.

Data Availability Statement

The data supporting this study's findings are available from the corresponding author upon reasonable request.

Animal Welfare

The authors confirm that they have adhered to ARRIVE Guidelines to protect animals used for scientific purposes.

References

1. **Baghezza S, Mamache B, Bennoune O, et al** (2021): *Pathological study and detection of Bovine parainfluenza 3 virus in pneumonic sheep lungs using direct immunofluorescence antibody technique.* Comp Clin Path, **30**, 301–310.
2. **Benavides J, González L, Dagleish M, et al** (2015): *Diagnostic pathology in microbial diseases of sheep or goats.* Vet Microbiol, **181**, 15-26.
3. **Caswell JL, Williams KJ** (2015): Respiratory system. 465–591. In: MG Maxie (Ed), Jubb, Kennedy and Palmer's Pathology of Domestic Animals, Volume 2, 6th ed. Elsevier, St. Louis, Missouri.
4. **Chakraborty S, Kumar A, Tiwari R, et al** (2014): *Advances in diagnosis of respiratory diseases of small ruminants.* Vet Med Int, **2014**, 508304.
5. **Chan S, Filézac de L'Etang A, Rangell L, et al** (2018): *A method for manual and automated multiplex RNAscope in situ hybridization and immunocytochemistry on cytospin samples*. Plos One, **13**, e0207619.

6. **Çeribaşı AO, Ozkaraca M, Çeribaşı S, et al** (2014): *Histopathologic, immunoperoxidase and immunofluorescent examinations on natural cattle pneumonia originated from Parainfluenza type 3, Respiratory Syncytial virus, Adenovirus type 3 and Herpesvirus type 1*. Rev Med Vet, **165**, 201-212.
7. **Durham PJ, Stevenson BJ, Farquharson BC** (1979): *Rotavirus and coronavirus associated diarrhoea in domestic animals.* N Z Vet J, **27**, 30–32.
8. **Heller MC, Chigerwe M** (2018): *Diagnosis and treatment of infectious enteritis in neonatal and juvenile ruminants.* Veterinary Clinics: Food Animal Practice, **34**, 101-117.
9. **Hindson JC, Winter A** (2008): Manual of sheep diseases, 2nd edition. John Wiley & Sons.
10. **Holmøy IH, Waage S, Granquist EG, et al** (2017): *Early neonatal lamb mortality: postmortem findings*. Animal, **11**, 295-305.
11. **Jarikre TA, Emikpe BO** (2017): *First report of immunohistochemical detection of Peste des petit ruminants, parainfluenza 3 and respiratory syncytial viral antigens in lungs of Nigerian goats.* J Immunoassay Immunochem, **38**, 555–568.
12. **Martella V, Decaro N, Buonavoglia C** (2015): *Enteric viral infections in lambs or kids.* Vet Microbiol, **181**, 154-160.
13. **Munday JS, Bentall H, Aberdein D, et al** (2020): *Death of a neonatal lamb due to Clostridium perfringens type B in New Zealand.* N Z Vet J, **68**, 242–246.
14. **Ozmen O, Yukari BA, Haligur M, et al** (2006): *Observations and immunohistochemical detection of Coronavirus, Cryptosporidium parvum and Giardia intestinalis in neonatal diarrhoea in lambs and kids.* Schweiz Arch Tierh, **148**, 357–364.
15. **Ozmen O, Haligur M, Aydogan A, et al** (2018): *Immunohistochemical detection of viral etiopathogenesis in lambs and goat kids with neonatal diarrhea*. Acta Sci Vet, **46**, 8.
16. **Sheehan M, Cassidy JP, Brady J, et al** (2007): *An aetiopathological study of chronic bronchopneumonia in lambs in Ireland*. Vet J, **173**, 630–637.
17. **Terzi OS, Kara E, Şenel Y, et al** (2022): *Dynamic thiol-disulphide homeostasis and ischemia modified albumin levels in neonatal calf diarrhea*. Ank Univ Vet Fak Derg, **70**, 81-86.
18. **Uzal FA, Plattner BL, Hostetter JM** (2015): Alimentary system. 1–257. In: MG Maxie (Ed), Jubb, Kennedy and Palmer's Pathology of Domestic Animals, Volume 2, 6th edn. Elsevier, St. Louis, Missouri.
19. **Yener Z, Sağlam YS, Timurkaan N, et al** (2005): *Immunohistochemical detection of parainfluenza type 3 virus antigens in paraffin sections of pneumonic caprine lungs.* J Vet Med A Physiol Pathol Clin Med, **52**, 268–271.